Polymer (Korea) Vol. 16, No. 4, pp 375－382 (1992)

고 변형률 속도하에서의 폴리카아보네이트의 동적 물성 결정을 위한 봉 충격 시험법에 있어서 종횡비의 효과

민 옥 기·남 창 훈*·이 정 민*
연세대학교 기계설계학과·*연세대학교 기계공학과
(1992년 1월 6일 접수)

Effect of Aspect-Ratio in Rod Impact Test for the Determination of Dynamic Material Properties of Polycarbonate at High-Strain-Rate

Oak-Key Min, Chang-Hoon Nam*, and Jeong-Min Lee*
Department of Mechanical Design & Production Engineering, Yonsei University, Seoul 120-749, Korea
**Department of Mechanical Engineering, Yonsei University, Seoul 120-749, Korea*
(Received January 6, 1992)

요 약 : 고 변형률 속도하에서 폴리카아보네이트의 동적 물성 결정을 위한 봉 충격 시험법에 있어서 종횡비의 효과에 대하여 연구하였다. 동적 물성의 계산을 위한 기초 데이타는 종횡비 범위 2～5인 끝면이 평면인 원통형 시험편을 공압 장치에 의하여 속도 범위 150～250 m/sec로 충돌시켜 얻었다. 동적 특성은 탄소성 파동 전파 이론에 의하여 계산하였다.

폴리카아보네이트의 동적 특성은 종횡비에 의존하며 그 효과는 종횡비가 증가함에 따라 감소한다. 일차원 개념을 이용한 이론을 타당하게 적용하려면 상대적으로 고 종횡비를 갖는 시험편을 사용하여 실험하여야 한다. 한편 봉 충격 시험에 의하여 도출된 폴리카아보네이트의 동적 항복 응력은 변형률 속도 범위 10^3～10^5 sec^{-1}에서 급격한 증가를 나타낸다.

Abstract : Effect of aspect-ratio in rod impact test for the determination of dynamic material properties of polycarbonate at high-strain-rate has been investigated. Data for the calculation of dynamic material properties have been obtained with flat-ended cylindrical rod specimens having aspect-ratios from 2 to 5, in the range of impact velocity from 150 to 250 m/sec by a compressed-air system. The calculation has been performed by theories based on one-dimensional elastic-plastic wave propagation phenomena.

The dynamic material properties of polycarbonate are dependent on the aspect-ratio and the effect diminishes with the increase of aspect-ratio. For the valid application of theories which use the concept of one-dimensionality, rod impact test should be performed by using the rod specimen having relatively high aspect-ratio. The dynamic yield stress determined by rod impact test shows the abrupt increase in the range of strain-rate 10^3～10^5 sec^{-1}.

INTRODUCTION

Polymers are being increasingly used in engineering applications where their behaviors under impact loading are of primary importance. In order to analyze accurately the deformation behavior and develop polymers having high-resistance against impact loading, characteristics and behaviors under high-strain-rate must be thoroughly investigated using appropriate testing techniques.

The testing techniques at high-strain-rate are well reviewed in numerous literatures.[1~4] Especially for compression, drop-weight test, Hopkinson pressure bar test, and rod impact test have been used.

Rod impact test is one of the simplest methods that can provide high-strain and high-strain-rate which cannot be obtained in other experimental techniques. In rod impact test the geometrical features of flat-ended cylindrical rod before and after the impact on flat rigid anvil are used as data for the determination of dynamic material properties. The dynamic material properties are determined through the analyses based on one-dimensional momentum and/or energy conservation theory[5~9] for metals, one-dimensional elastic-plastic wave propagation theory[10~11] for polymers, and two-dimensional dynamic nonlinear finite element/difference codes.[12~14]

Since rod specimens having various ratio of length to diameter(aspect-ratio) can be used in rod impact test, the effects of aspect-ratio on the determination of dynamic material properties must be investigated in order to obtain reliable results. Although the effects of aspect-ratio have been discussed for metals in some papers,[7~9,15~16] whereas not for polymers.

In the present study, the effects of aspect-ratio have been investigated for polycarbonate(PC) by performing rod impact test which uses a compressed-air system for acceleration of the flat-ended cylindrical rod specimens having various aspect-ratios from 2 to 5. From the geometrical measurements of rod specimens before and after the impact on rigid anvil, the dynamic material properties of PC have been determined for each aspect-ratio through the analyses based on one-dimensional elastic-plastic wave propagation theories which have been proposed by previous workers.[10~11]

REVIEW OF PREVIOUS THEORY

Consider a uniform rod of initial dimensions, length L and cross-sectional area A, that impacts on a rigid anvil with impact velocity V as shown in Fig. 1(a). Assuming that V is large enough, a portion of the rod will deform plastically. At time t after the impact, the rod will deform as shown in Fig. 1(b), where h the deformed length, x the undeformed length, s the displacement of rod. And at the end of impact, the rod has the final deformed length H, the final undeformed length X, and the final total length L_f.

Hutchings[10] and Date[11] used following assumptions for the calculation of dynamic material properties.

- One-dimensional elastic-plastic wave propagation is considered.
- The deformation of rod takes place at a constant strain rate.
- The stress-strain relationship of a material is the same throughout the duration of impact.
- A linearly-elastic, perfectly-plastic material is assumed.

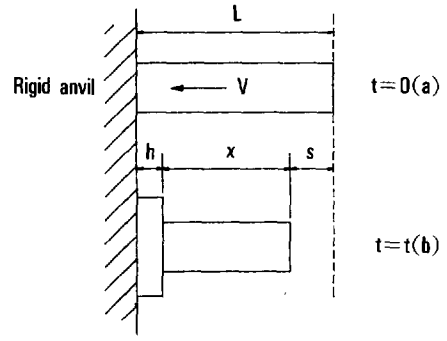

Fig. 1. The process of deformation of flat-ended cylindrical rod impinging on rigid anvil.

◦ The elastic unloading has the same modulus as that for loading.

When impact with plastic deformation occurs, the elastic wave and plastic wave are simultaneously propagated from the interface between the impinging rod and the anvil ; they travel outwards along the rod at velocity C_o and C_p, respectively. By considering an element of the material it may be deduced from the condition of momentum balance that

$$\Delta\sigma=\rho C\Delta v \tag{1}$$

where ρ is material density, $\Delta\sigma$ and Δv are infinitesimal changes in nominal stress and particle velocity, and C is the wave velocity in terms of Lagrangian coordinates. The changes in nominal strain Δe and particle velocity Δv are related by

$$\Delta v=C\Delta e \tag{2}$$

From equations (1) and (2) the wave velocity is given by

$$C^2=(\Delta\sigma/\Delta e)/\rho \tag{3}$$

and then elastic wave and plastic wave will propagate with velocities

$$C_o=(\sigma_y/\rho e_y)^{1/2} \tag{4}$$

$$C_p=[(\sigma-\sigma_y)/\rho(e-e_y)]^{1/2} \tag{5}$$

where σ_y and e_y are nominal yield stress and nominal yield strain, respectively.

Since the particle velocity behind a plastic wave front is zero, the nominal stress behind the plastic wave front becomes

$$\sigma=\rho C_p V+\sigma_y[1-(C_p/C_o)] \tag{6}$$

from equations (1) and (4).

Where since the nominal stress $\sigma(\geq\sigma_y)$ and the true stress Y are related by

$$Y=\sigma(1-e) \tag{7}$$

equations (4)~(6) become

$$C_o=[Y/(\rho e_y(1-e_y))]^{1/2} \tag{8}$$

$$C_p=[Y/(\rho(1-e)(1-e_y))]^{1/2} \tag{9}$$

$$\sigma=\rho C_p V+Y[1-(C_p/C_o)]/(1-e_y) \tag{10}$$

With the assumptions described above, Hutchings assumed additionally that the plastic wave front does stop at the first elastic wave interaction. Then the position of plastic wave front may be deduced in the terms of the measured fractional reduction in length of rod k defined as

$$k=1-(L_f/L) \tag{11}$$

Since the residual strain in the region which the plastic wave front has traversed is $(e-e_y)$,

$$k=2\overline{C_p}(e-e_y)/(1+\overline{C_p}) \tag{12}$$

where $\overline{C_p}=C_p/C_o=[e_y/(1-e)]^{1/2}$ from equations (8) and (9). If we substitute $\overline{C_p}$ into equation (12),

$$e=\{(8e_y^2+4ke_y-k^2)+[(k^2-8e_y^2-4ke_y)^2 -16e_y(4e_y^3+4ke_y^2+k2e_y-k^2)]^{1/2}\}/8e_y \tag{13}$$

And from equation (10) substituted by equations (7)~(9), we obtain

$$(Y/\rho V^2)^{1/2}=\overline{C_p}/\{(e_y-e_y^2)^{1/2}[1/(1-e)-(1-\overline{C_p})/(1-e_y)]\} \tag{14}$$

where $\overline{C_p}$ is given by $[e_y/(1-e)]^{1/2}$ and e by equation (13).

For a second relationship between the two unknowns Y and e_y, Hutchings used the critical impact velocity V_c below which the deformation is purely elastic. From equation (10)

$$\sigma_y=\rho C_o V_c \tag{15}$$

And from equations (7) and (8), equation (15) becomes

$$e_y=(\rho V_c^2/Y)/[1+(\rho V_c^2/Y)] \tag{16}$$

From measurements of V_c, ρ, V and k the values of e_y and Y may be determined by using equations (14) and (16).

The foregoing analysis provides a means of estimating the dynamic yield stress and strain from measurements of the changes in length of a rod due to impact at a known velocity, and a knowle-

dge of the critical impact velocity for the onset of plastic deformation. However for the analysis to remain valid, the condition must be satisfied that the plastic wave front must be wholly attenuated at the first elastic wave interaction. And the limit impact velocity which is the maximum velocity to permit the analysis to remain valid, can be shown such as

$$V_1 = C_o e_y [1 + 2C_o/(C_o + C_p)] \quad (17)$$

because the unloaded plastic region should have the dynamic yield strain as maximum strain.

Meanwhile Date performed rod impact test for the determination of dynamic material properties of polyvinylchloride in which rod collides with an elastic bar, and observed that contact time is constant even though impact velocity is over the limit impact velocity. From the experimental results, Date assumed the elastic wave velocity is constant and used following equation instead of equation (16).

$$C_o^2 = \sigma_y/(\rho e_y) = \text{constant} \quad (18)$$

where static elastic modulus was used for the calculation of C_o. Similar with Hutchings' theory, from measurements of ρ, V, and k the values of Y and e_y may be determined by using equations (14) and (18).

For the strain-rate Hutchings and Date used following equation proposed by Taylor.[5]

$$\dot{e} = V/[2(L - X)] \quad (19)$$

EXPERIMENT

Test Material

The material of specimen used in the rod impact test is polycarbonate(PC) which has the physical properties as shown in Table 1. Rod specimens have been machined to have a flat-ended cylindrical shape of various aspect-ratios(L/D ; L and D are length and diameter of rod, respectively) from 2 to 5 as shown in Fig. 2.

Experimental Setup

Rod impact test has been performed using the experimental setup shown in Fig. 3, which consists of the compressed-air system, the air release system, the accelerating tube, the velocity measurement system, and the rigid flat anvil.

Table 1. Physical Properties of PC

Density(ρ) (kg/m^3)	Compressive modulus(E)* (MPa)
1.196×10^3	2.4×10^3

* From reference 17

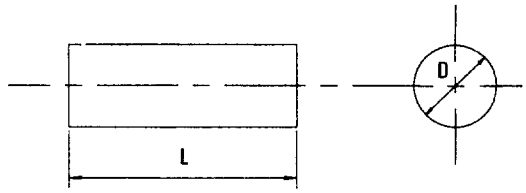

Aspect-ratio(L/D)	Length(L) (mm)	Diameter(D) (mm)
2.0	$20^{+0.05}_{-0.05}$	$10^{+0.00}_{-0.05}$
3.0	$30^{+0.05}_{-0.05}$	$10^{+0.00}_{-0.05}$
4.0	$40^{+0.05}_{-0.05}$	$10^{+0.00}_{-0.05}$
5.0	$50^{+0.05}_{-0.05}$	$10^{+0.00}_{-0.05}$

Fig. 2. Shape of rod specimen of PC.

The rod specimen has been accelerated by a compressed-air system in the pressure range from 0 to 10 MPa where the required pressure is obtained using air control units including compressor, reservoir, regulator,and accumulator. For the normal impact of rod specimens, the cylindrical accelerating tube has been used, which has the length of 1 m and the interior diameter of 10 mm. The compressed- air is released to the accelerating tube by an air release system which consists of ball valve and the rupture diaphragm made of copper membrane. The velocity of impact has been determined by using the photoelectronic sensors which utilize Red Led light beam and time counter(Racal Dana Model 9015/11A). The impact velocity can be calculated from the flight time and the distance between light beams. The used range of impact velocity is 150~250 m/sec.

Meanwhile in order to measure the geometrical

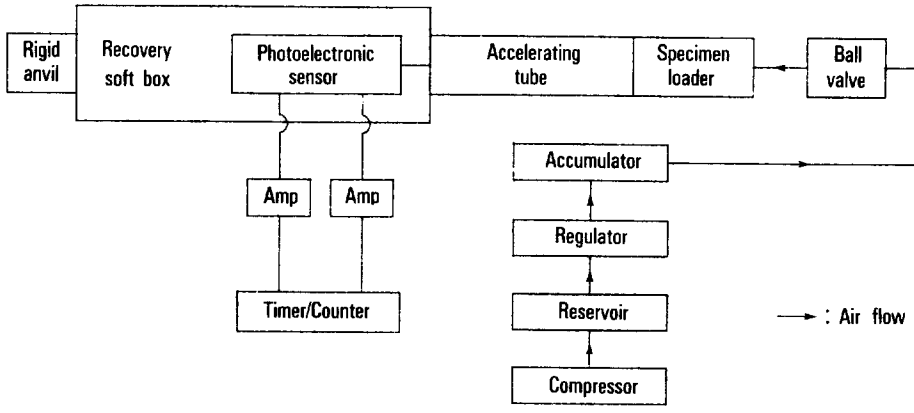

Fig. 3. Experimental setup for rod impact test.

features of rod specimen after the impact, a recovery box has been installed ahead the rigid flat anvil which is the electroslag remelted wrought-steel homogeneous plate having the hardness of HB500. The anvil has been fixed by rigid structure on the ground in order to prevent the movement of the anvil.

After the impact the deformed specimen has been thoroughly inspected in order to choose the specimen to be analyzed. When the fracture, the nonaxisymmetrical deformation, and the buckling occur, the specimen has been excluded in the analysis. And then the shape of the deformed specimen has been enlarged by the profile projector, and the geometrical features such as final undeformed length, final deformed length, and final total length have been accurately measured by the mechanical devices.

Experimental Results

From the geometrical measurements of deformed rod, the variation of nondimensionalized final total length L_f/L with impact velocity V has been plotted for each aspect-ratio as shown in Fig. 4, where L_f/L decreases linearly with the increase of impact velocity as observed in previous works.[10,18] As can be seen from Fig. 4, when the aspect-ratio increases, L_f/L decreases with the decreasing level. This means that the dynamic material properties of PC are dependent on the aspect-ratio and

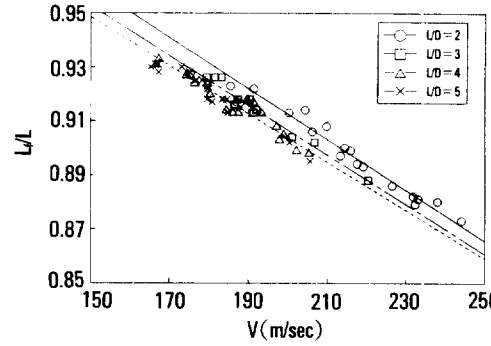

Fig. 4. Variation of nondimensionalized final total length(L_f/L) with impact velocity(V) for PC having various aspect-ratio(L/D).

the effect diminishes with the increase of aspect-ratio.

For the calculation of dynamic material properties using the theory proposed by Hutchings,[10] critical impact velocity V_c has been determined from the relation between the fractional reduction in length k and the impact velocity as shown in Fig.5. Where V_c has been determined when k becomes zero, and tabulated in Table 2, in which V_c decreases with the increase of aspect-ratio from 107.2 to 89.3 m/sec. And for the calculation of dynamic material properties using the theory proposed by Date, the static compressive elastic modulus E has been used from Chanda and Roy.[17]

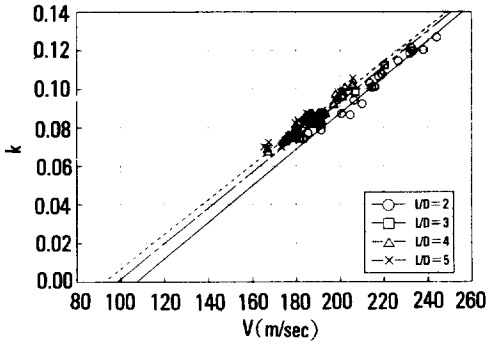

Fig. 5. Relation between fractional reduction in length (k) and impact velocity(V) for PC having various aspect-ratio(L/D).

Table 2. Critical Impact Velocity(V_c) of PC along the Aspect-Ratio(L/D)

Material	L/D	V_c(m/sec)
Polycarbonate	2.0	107.2
	3.0	98.3
	4.0	92.3
	5.0	89.3

ANALYSIS AND DISCUSSION

On the basis of one-dimensional elastic-plastic wave propagation theories proposed by Hutchings [10] and Date,[11] the dynamic yield stress Y and the dynamic yield strain e_y of PC have been calculated. Variations of dynamic yield stress and strain with impact velocity is shown in Fig. 6~9 for each theory and aspect-ratio. Hutchings' theory which uses critical impact velocity as an input parameter, shows larger dispersions in dynamic yield stress and strain for each aspect-ratio than Date's theory which uses static elastic modulus as an input parameter.

The average dynamic yield stress and strain are shown in Table 3. Hutchings' theory shows higher dynamic yield stress and lower dynamic yield strain than Date's theory. For the two theories dynamic material properties are dependent on the aspect-ratio and the effect diminishes with the increase of aspect-ratio. This seems to result from the

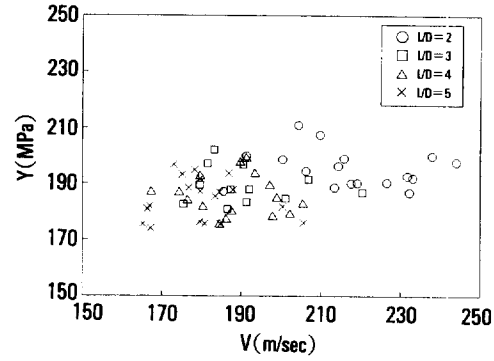

Fig. 6. Variation of dynamic yield stress(Y) with impact velocity(V)(hutchings' theory).

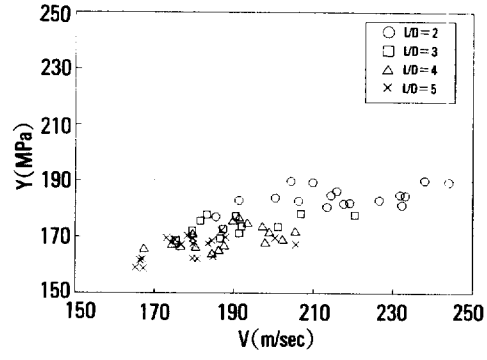

Fig. 7. Variation of dynamic yield stress(Y) with impact velocity(V)(date's theory).

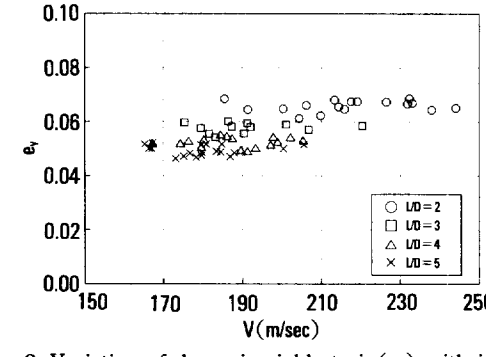

Fig. 8. Variation of dynamic yield strain(e_y) with impact velocity(V)(hutchings' theory).

radial inertia effect in the rod specimen having relatively short aspect-ratio. Hence for the valid application of theories which use the concept of one-dimensionality, rod impact test should be perfor-

Table 3. Variation of Dynamic Yield Stress(Y), Dynamic Yield Strain(e_y), and Strain Rate($\dot{e}$) with Aspect-Ratio (L/D)

L/D	Hutchings' theory		Date's theory		$\dot{e}$
	Y(MPa)	e_y	Y(MPa)	e_y	($\times 10^3 sec^{-1}$)
2.0	195.36	0.0658	184.36	0.0833	11.364
3.0	189.18	0.0577	173.90	0.0782	7.309
4.0	185.51	0.0522	169.45	0.0760	5.325
5.0	184.39	0.0492	166.16	0.0744	4.289

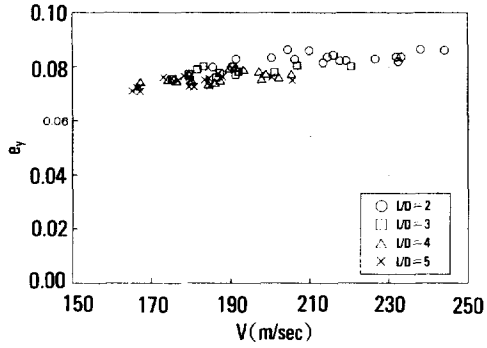

Fig. 9. Variation of dynamic yield strain(e_y) with impact velocity(V)(date's theory).

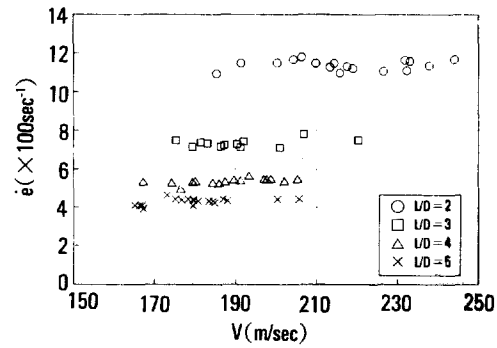

Fig. 10. Variation of strain rate($\dot{e}$) with impact velocity(V).

med by using the rod specimen having relatively high aspect-ratio.

For the two theories, the variation of the calculated strain-rate with impact velocity is shown for each aspect-ratio in Fig. 10, where the strain-rate is constant with impact velocity and decreases with the increace of aspect-ratio. The average values are tabulated in Table 3, where the strain-rate decreases from 11.364×10^3 to 4.289×10^3 sec^{-1}.

Rod impact tests for the determination of dynamic material properties of engineering polymers have been performed by various workers.[10~11,18~19] Especially Kukureka and Hutchings[18] performed rod impact test of PC having aspect-ratio of 2.5, and found that the critical impact velocity V_c is 104 m/s, the dynamic yield stress Y is 174 MPa, the dynamic yield strain e_y is 0.069, and the strain rate is $6\sim7\times10^3$ at room temperature. The present results are similar with Kukureka and Hutchings' results.

Meanwhile Kukureka and Hutchings[20] investi-

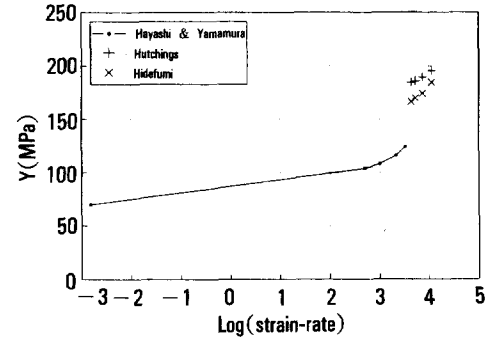

Fig. 11. Relation between dynamic yield stress(Y) and log(strain-rate) for PC.

gated the mechanical response of engineering polymers to dynamic compressive loading by a block-bar impact machine at strain-rates in the range of 100 to 500 sec^{-1}, and found that the dependence of yield stress on log(strain-rate) is approximately linear for used materials including PC, while noted that at some point the dependency of yield stress on log(strain-rate) ceases to be linear. The abrupt

increase of yield stress is also found in Hayashi and Yamamura's paper[21] which used Hopkinson pressure bar test. The insertion of the present results into the Hayashi and Yamamura's results for the variation of yield stress with log(strain-rate) of PC is shown in Fig. 11, where the abrupt increase of yield stress can be seen.

CONCLUSIONS

Effect of aspect-ratio in rod impact test for the determination of dynamic material properties has been investigated for polycarbonate by performing rod impact test which uses a compressed-air system for the acceleration of flat-ended cylindrical rod specimens having aspect-ratios from 2 to 5 in the range of impact velocity from 150 to 250 m/sec. From the geometrical measurements of rod specimens before and after the impact on rigid anvil, the dynamic material properties have been determined for each aspect-ratio through the analyses based on one-dimensional elastic-plastic wave propagation theories which have been proposed by previous workers.

1. The dynamic material properties of polycarbonate are dependent on the aspect-ratio and the effect diminishes with the increase of aspect-ratio.

2. For the valid application of theories which use the concept of one-dimensionality, rod impact test should be performed by using the rod specimen having relatively high aspect-ratio.

3. The dynamic yield stress determined by rod impact test shows the abrupt increase in the range of strain-rate 10^3-10^5 sec^{-1}.

Acknowledgement : This work was supported by a Yonsei University Faculty Research Grant for 1992.

REFERENCES

1. J. Harding, "Testing techniques at high rates of strain", OUEL-1308180, University of Oxford, 1980.
2. M.R.Staker et al., "High strain rate testing", in Matals Handbook, Ninth Edition, Vol. 8, American Society for Metals, 1985.
3. J. A .Zukas et al., "Impact dynamics", John Wiley & Sons, 1982.
4. J. A. Zukas, "High velocity impact dynamics", John Wiley & Sons, 1990.
5. G. I. Taylor, *Proc. R. Soc.*, **A194**, 289 (1948).
6. J. B. Hawkyard, *Int. J. Mech. Sci.*, **11**, 313 (1969).
7. P. P. Gillis et al., *J. Appl. Phys.*, **61**, 499 (1987).
8. P. P. Gillis et al., *Mech. Mat.*, **6**, 293 (1987).
9. P. P. Gillis and S. E. Jones, *J. Eng. Mat. Tech.*, **111**, 327 (1989).
10. I. M. Hutchings, *J. Mech. Phys. Solids*, **26**, 289 (1979).
11. H. Date, *J. Soc. Mat. Sci.(Japan)*, **33**, 1482 (1984).
12. M. L. Wilkins and M. W. Guinan, *J. Appl. Phys.*, **44**, 1200 (1973).
13. G. R. Johnson and T. J. Holmquist, *J. Appl. Phys.*, **64**, 3901 (1988).
14. F. J. Zerilli and R. W. Armstrong, *J. Appl. Phys.*, **61**, 1816 (1987).
15. R. P. Papirno, Proc. Army Sym. on Solid Mechanics, AMMRC MS 80-4, p. 367, 1980.
16. J. W. House, "Taylor impact testing", AFATL-TR-89-41, 1989.
17. M. Chanda and S. K. Roy, "Plastics technology handbook", p. 526, Marcel Dekker, 1987.
18. S. N. Kukureka and I. M. Hutchings, Proc. 7th Int. Conf. on High Energy Rate Febrication, University of Leeds, p. 29, 1981.
19. B. J. Briscoe and I. M. Hutchings, *Polymer*, **17**, 1099 (1976).
20. S. N. Kukureka and I. M. Hutchings, *Int. J. Mech. Sci.*, **26**, 617 (1984).
21. T. Hayashi and H. Yamamura, *Trans. JSME*, **A46**, 1096 (1980).